communications earth & environment

A Nature Portfolio journal

Article

https://doi.org/10.1038/s43247-025-02577-7

Aerosol-driven North Pacific High anomaly enhances sea ice loss in the Chukchi Sea

Check for updates

Yungi Hong [1], S.-Y. Simon Wang [2] & Jin-Ho Yoon [1]

The Arctic has warmed significantly faster than the rest of the globe, leading to rapid sea ice decline. Anthropogenic aerosols are traditionally viewed as cooling agents that do not contribute to Arctic sea ice loss. Here we investigate how aerosol-induced changes in atmospheric circulation patterns contribute to Arctic sea ice decline using a fully-coupled global earth system model. We compared single forcing experiments to examine individual and combined effects of greenhouse gases and anthropogenic aerosols. Aerosols contribute to intensification of the North Pacific anticyclone, which enhances heat transport into the Arctic through the Bering Strait. When combined with greenhouse gas-induced warming, aerosols have a greater impact on Arctic sea ice decline in the western Chukchi Sea compared to when either forcing acts independently. This compound effect challenges the traditional view of aerosols as solely cooling agents, demonstrating that anthropogenic aerosols can accelerate Arctic sea ice melting.

The Arctic Amplification (AA) phenomenon, where the Arctic warms faster than the rest of the world, has become a key topic in climate change discussions due to its divergent impact[1]. Recent observations indicate that the Arctic has warmed at nearly four times the rate of the global average since 1979[2], with this enhanced warming particularly pronounced in autumn and winter[3]. While the ice-albedo feedback is considered the primary cause of AA[4], the regional contrasts in sea ice loss suggest that various atmospheric, oceanic, and surface processes also play critical roles[5–9].

The drivers of Arctic amplification encompass both local and remote mechanisms[1]. Beyond the well-established ice-albedo feedback, local processes include temperature-related feedbacks such as the lapse-rate feedback, whereby the stably stratified Arctic atmosphere retains more warming compared to lower latitudes[10]. Remote mechanisms involve enhanced poleward heat transport through both atmospheric and oceanic pathways. Recent research has documented significant increases in oceanic heat fluxes into the Arctic, particularly through the Atlantic gateway via the Norwegian and Barents Seas, as well as through the Pacific gateway via the Bering Strait[11,12]. These increased heat fluxes have been shown to substantially delay sea ice reformation and weaken Arctic halocline stratification, allowing deeper heat to reach the surface and intensify ice loss[13].

Among the Arctic regions, the Chukchi Sea, where it serves as the critical Pacific-Arctic gateway and contributes disproportionately to Arctic amplification stands out for its particularly rapid warming and sea ice loss (Fig. 1a), making it a key area of concern in the Arctic climate change[14]. Climate projections suggest that, by 2050, the Bering Sea will experience temperature increases exceeding 3 °C, while the neighboring Chukchi Sea is expected to see a rise of around 5 °C[15]. This outstanding warming in the Bering Sea is linked to increased ocean heat transport through the Bering Strait, which accelerates sea ice loss in the Chukchi Sea[16]. Furthermore, changes in atmospheric circulation, such as atmospheric blocking over the Bering Sea, have been observed to increase this heat transport that is contributing to sea ice decline[17]. Episodic atmospheric blocking patterns over the Bering Sea generate anomalous southerly winds that significantly delay sea ice formation by increasing warm water transport. Moreover, pressure pattern variations between the Beaufort High and Aleutian Low systems are particularly influential, as they drive surface wind anomalies that control warm water transport through the Bering Strait and influence sea ice variability in the Pacific Arctic region[18].

The regional heterogeneity of Arctic warming and sea ice loss is a defining characteristic of Arctic amplification. While the Barents-Kara Seas region has historically shown the most pronounced warming in the Atlantic sector[19], the Chukchi and Beaufort Seas have experienced dramatic sea ice reduction in the Pacific sector[20]. This spatial variability highlights the complex interplay between local feedbacks and large-scale heat transport mechanisms that cannot be explained by greenhouse gas forcing alone. Understanding this regional variability is crucial for accurate climate projections and for identifying the diverse mechanisms driving Arctic change.

While greenhouse gases (GHG) have long been recognized as the primary driver of AA, the role of anthropogenic aerosols (AAER) in Arctic sea ice decline remains understudied, partly due to their overall cooling effect. Recent studies suggest, however, that AAER can influence

[1]Department of Environment and Energy Engineering, College of Engineering, Gwangju Institute of Science and Technology, Gwangju, South Korea. [2]Department of Agronomy, Kasetsart University, Bangkok, Thailand. e-mail: yjinho@gist.ac.kr

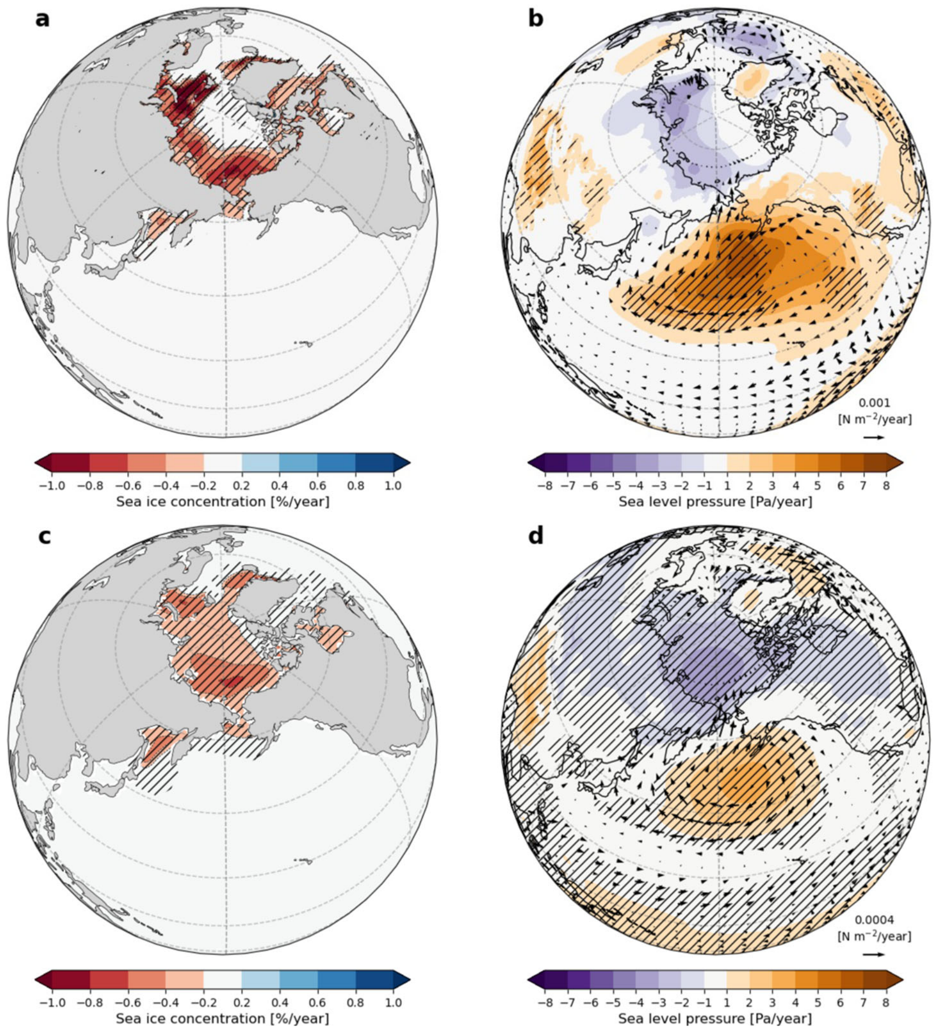

Fig. 1 | Annual trend maps for the period 1980–2020. Annual trend maps of (**a**, **c**) sea ice concentration and (**b**, **d**) mean sea-level pressure (shading) & surface stress (vectors) for the period 1980–2020 in (**a**, **b**) ERA5 and (**c**, **d**) CESM2-All simulation. Hatched regions indicate areas where the trends are statistically significant ($p < 0.05$).

atmospheric circulation patterns in higher latitudes, such as weakening the North Pacific storm track, which may increase northward heat transport[17,21]. Asian aerosols can induce stationary Rossby waves that propagate across the Pacific, modifying atmospheric circulation patterns through the displacement of pressure systems and alteration of jet stream configurations[21,22]. These circulation changes could have significant implications for Arctic sea ice, yet the specific contribution of AAER to sea ice loss remains unexplored.

This research examines the synergistic effects of AAER and GHG on ocean heat flux through the Bering Strait and their combined impact on sea ice loss. Our CESM2 large ensemble analysis ("Methods" for detail) demonstrates that AAER-driven changes in North Pacific circulation can significantly explain the observed trends, even leading to an enhancement of northward heat transport that counteracts cooling effects. Moreover, when acting together with GHG, these processes are shown to intensify sea ice decline. This study bridges two established research areas: the influence of North Pacific circulation changes on Arctic sea ice and the effect of anthropogenic aerosols on North Pacific circulation patterns. Being the first to examine these connections together, we show that aerosols contribute to Arctic sea ice loss through their impact on regional atmospheric dynamics, a relationship that has received limited attention in previous research. Our findings challenge the conventional understanding of aerosols as purely cooling agents while highlighting the complex interactions between GHG, AAER, and regional atmospheric dynamics.

Results

Arctic sea ice trends and associated circulation changes

The decline of Arctic sea ice over the past 40 years has been pronounced (Fig. 1a). In particular, the Chukchi and Barents-Kara Seas have shown significant sea ice loss compared to other regions. Concurrent with these sea ice changes, anomalous high pressure over the North Pacific paired with low pressure in the Arctic has been observed (Fig. 1b). These recent changes in sea ice and atmospheric circulation patterns are well mirrored in simulated climate by the CESM2 (Fig. 1c, d). Although the model underestimates the intensity of these changes, it reproduces the pronounced sea ice loss in the Chukchi and Barents-Kara Seas, as well as the positive and negative sea level pressure trends over the North Pacific and Arctic, respectively. Similar patterns are also captured in the multi-model mean from CMIP6 models for both sea ice concentration and sea level pressure (Fig. S1, Table S1). However, CESM2 shows better alignment with observations in representing both the regional intensity of sea ice decline and the spatial configuration of atmospheric circulation patterns. Additional comparison with observational datasets confirms that CESM2 realistically captures the seasonal cycle of Arctic sea ice extent and the spatial structure of sea level pressure (Figs. S2 and S3). This consistency lends credibility to the CESM2 simulations and supports our investigation of potential roles played by AAER in Arctic sea ice loss.

The sea ice concentration (SIC) trends in the All and GHG simulations (Methods) show consistent results, with widespread sea ice loss across most of the Arctic (Fig. S4). However, there is a notable underestimation of the

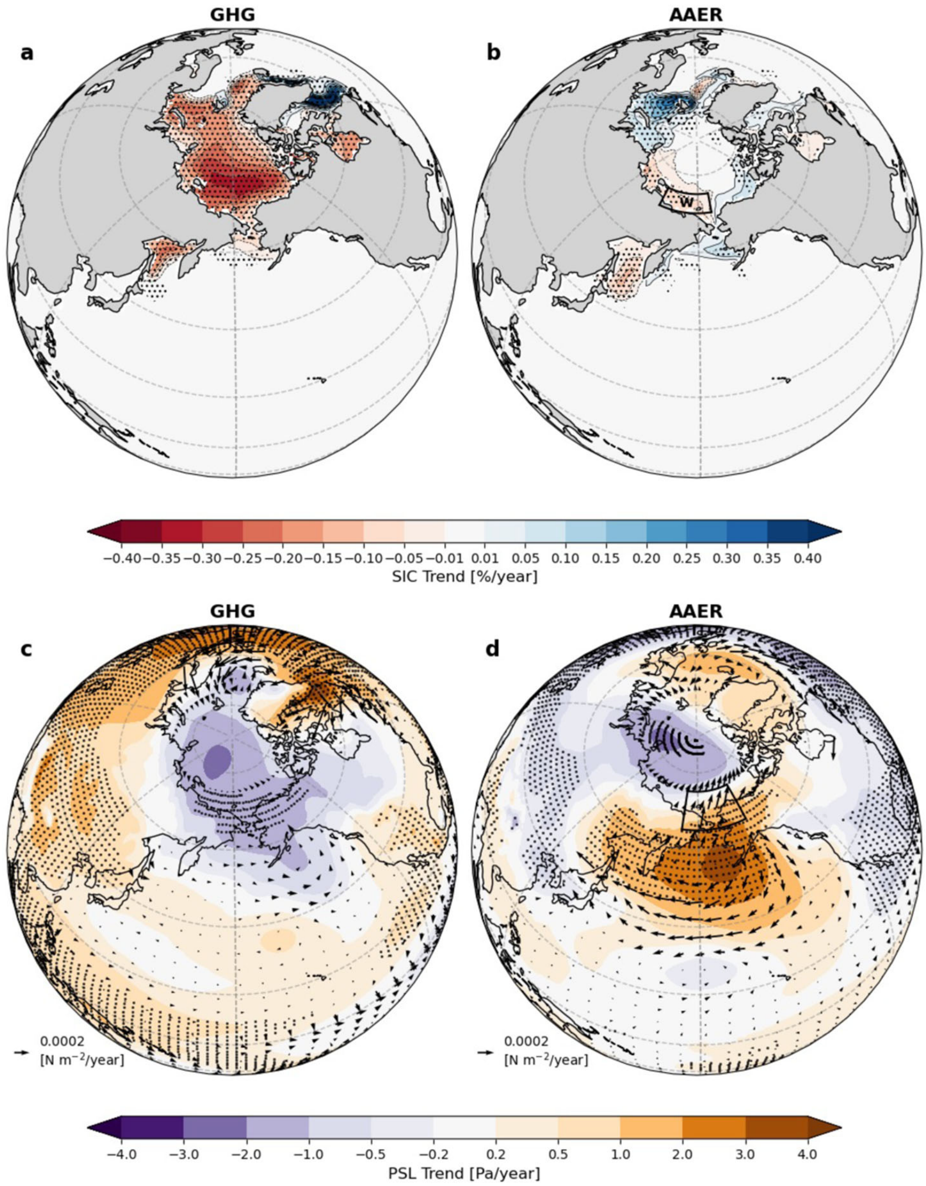

Fig. 2 | Annual trend maps for the period 1980–2020 in CESM2-GHG and CESM2-AAER simulations. Annual trend maps of (**a**, **b**) sea ice concentration and (**c**, **d**) mean sea-level pressure (shading) & surface stress (vectors) for the period 1980–2020. **a**, **c** show GHG, and **b**, **d** show AAER simulation results. The black box in (**b**) indicates the western Chukchi Sea (150°–190°E, 70°–75°N). The black box in (**d**) indicates the Bering Strait (170°–210°E, 65°–75°N). Hatched regions indicate areas where the trends are statistically significant ($p < 0.05$).

SIC decline in GHG-only forcing compared to the All-forcing one, indicating that additional forcings or processes act in the All forcing to accelerate sea ice melting. In contrast to the All and GHG simulations, the AAER simulation shows that most Arctic regions experience either an increase or no change in sea ice (Fig. 2b). However, the western Chukchi Sea and the Okhotsk Sea exhibit weak sea ice loss, suggesting that AAER may contribute to sea ice loss in certain areas, an undocumented phenomenon that is examined here.

By examining the trends in mean sea level pressure and surface stress, we note a dipole pattern of the circulation change, characterized by an anticyclone over the North Pacific and a cyclone over the Arctic (Fig. 1d). It is interesting to note that these features are almost evenly attributed to different single forcings: the cyclone over the Arctic is observed in the GHG simulation (Fig. 2c), while the anticyclone over the North Pacific appears in the AAER simulation (Fig. 2d). This dipole circulation, particularly the anticyclone over the North Pacific, weakens the storm track and induces northward ocean heat transport through the Bering Strait[17]. Because one of the factors that could contribute to sea ice loss in the Chukchi Sea is ocean heat transport through the Bering Strait[16,17], Fig. 2d suggests that AAER plays a much larger role than GHG in generating northward surface stress in the Bering Strait. This process can lead to ocean heat transport into the western Chukchi Sea, contributing to sea ice loss.

We validated these single-forcing results using additional CMIP6 DAMIP models with >10 ensembles (Table S2). CMIP6 DAMIP multi-model analysis confirms our CESM2 results (Figs. 2, S5, S6). All models show consistent North Pacific positive pressure trends under AAER forcing, validating the fundamental aerosol-circulation mechanism. However, regional sea ice responses depend on anticyclone positioning—enhanced northward transport requires Alaska-adjacent positioning[17,18]. This spatial sensitivity explains inter-model variability while confirming the robust underlying mechanism.

Linear and nonlinear components of Arctic change

Even though the All and GHG simulations show a similar pattern of sea ice loss, there is a significant discrepancy in the magnitude of that loss (Fig. S4). The absence of various interactions and feedbacks contributing to sea ice loss in the Arctic in any single-forcing simulation may explain why GHG underestimates sea ice loss. Therefore, we adopt a straightforward way to approximate the linear and nonlinear effects of the all simulations to estimate external forcing and other factors that could cause sea ice loss, including net effects of the feedback processes (see "Methods").

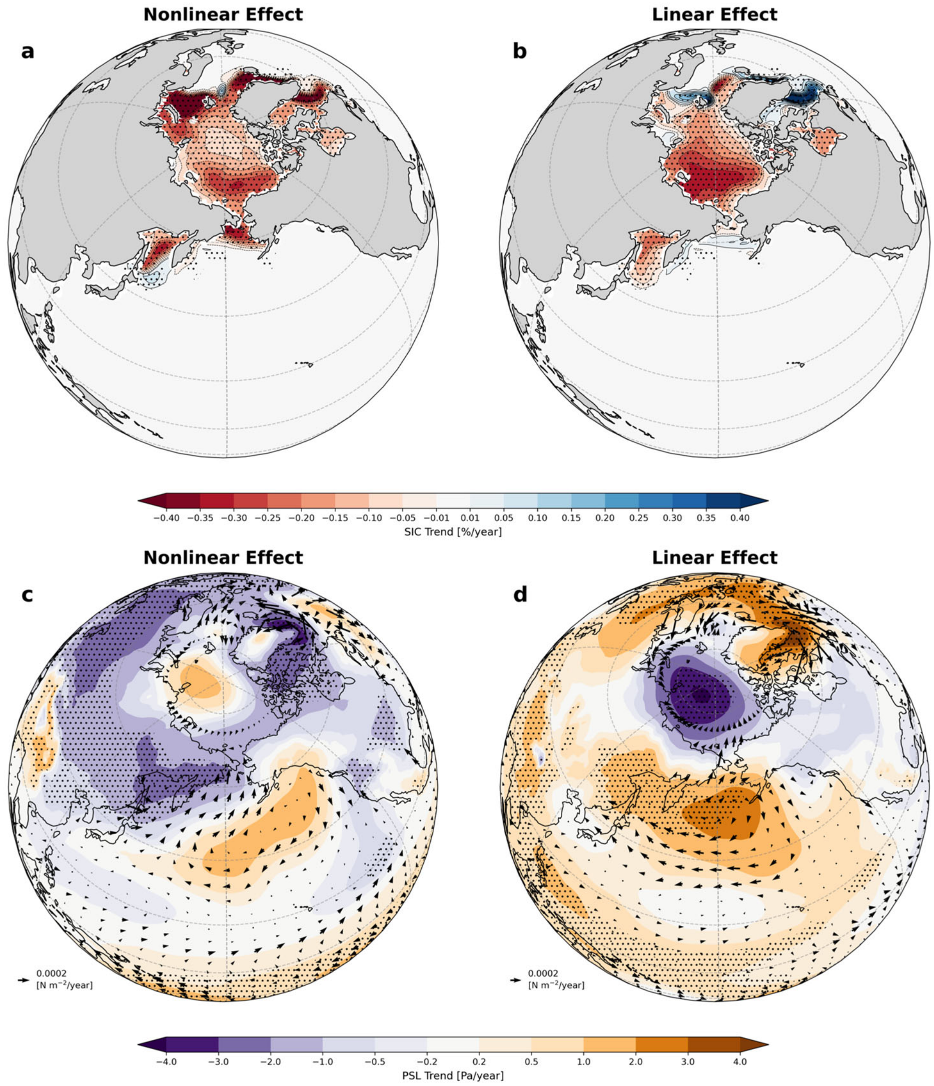

Fig. 3 | Nonlinear and linear effects on trends in Arctic sea ice and atmospheric parameters (1980–2020). Annual trend maps of (**a**, **b**) sea ice concentration and (**c**, **d**) mean sea level pressure (shading) & surface stress (vectors) for the period 1980–2020. **a**, **c** show nonlinear effect and (**b**, **d**) show linear effect. The linear effect is defined as the sum of the individual trends of GHG and AAER. The nonlinear effect is then calculated by subtracting this sum from the ALL simulation. Hatched regions indicate areas where the trends are statistically significant ($p < 0.05$).

Considering the linear effect (GHG + AAER; Fig. 3b), the western Chukchi Sea experiences more intense sea ice loss compared to the GHG simulations alone (Fig. 2a) as well as the nonlinear effect (Fig. 3a). This suggests that the compound effect of GHG and AAER carries more weight than nonlinear effects in the western Chukchi Sea, with AAER apparently amplifying GHG-induced sea ice loss. To quantify this compound effect, time series of western Chukchi Sea ice concentration were examined from the ALL forcing simulation, GHG-only simulation, and the combined GHG + AAER effect (Fig. S7). The combined GHG + AAER effect was calculated by summing the GHG and AAER simulations with an initial offset correction to ensure proper alignment with the ALL simulation. Variance partitioning analysis revealed that the GHG + AAER combination explains 4.4% more variance (R^2) than GHG forcing alone when comparing their explained variance relative to the ALL simulation. More notably, the GHG + AAER combination captures 52.08% of the total variance in the ALL simulation compared to just 29.15% for GHG-only, demonstrating the substantial improvement in representing sea ice variability when aerosol-induced circulation changes are included alongside greenhouse gas forcing.

Conversely, there is a relative increase in sea ice in the Barents Sea and Greenland (Fig. 3b), as AAER exerts a strong cooling and offset GHG-induced sea ice loss in these regions. Additionally, the weakened AMOC, supposedly driven by GHGs[23] contributes to the Arctic cooling by reducing northward heat transport in the Barents and Greenland Seas. Beyond the linear effect, it is reasonable to assume that the significant sea ice loss in the Barents and Greenland Seas observed in the All simulation can be mostly attributed to nonlinear effects (Fig. 3a). These findings suggest that nonlinear factors, such as feedback mechanisms and even natural forcing, play a role in the overall Arctic SIC decline, particularly in the Atlantic Arctic regions.

To further clarify the contribution of internal variability to these nonlinear effects, we conducted an additional analysis using our 50-member ensemble. Internal variability was computed as deviations from the ensemble mean and showed strong spatial heterogeneity, with particularly high variability in the Barents and Greenland Seas, as well as along the sea ice margins (Fig. S8). The magnitude and statistical significance of these deviations were further assessed, revealing that these regions exhibit both large standard deviations and a high fraction of ensemble members with significant anomalies (Fig. S9). This pattern highlights the susceptibility of marginal ice zones to internal variability and underscores its substantial role in shaping regional sea ice changes. These results provide valuable insights for interpreting the nonlinear components of Arctic sea ice decline.

The presence of these spatial contrasts in nonlinear behavior can also be traced in the circulation trends, inferring a dynamic process. The linear effect in mean sea level pressure and surface stress trends shows a dipole pattern similar to the All simulation, while the nonlinear effect shows a broad latitudinal difference between the polar circle and the mid-latitudes, instead reflecting the meridional thermal gradients in the warmer climate

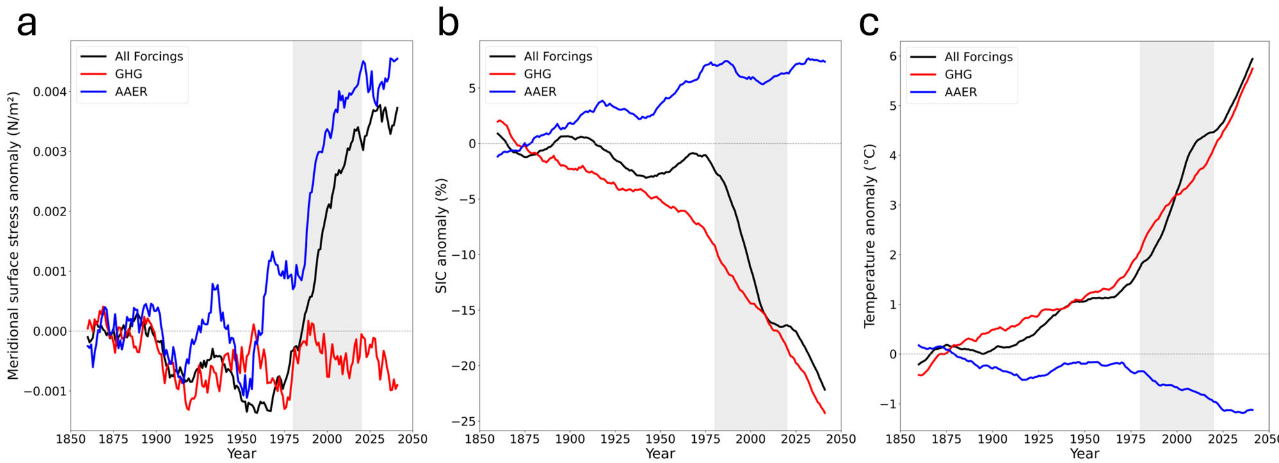

Fig. 4 | Time series of meridional surface stress, sea ice concentration, and temperature. Running 20-year anomaly time series of (**a**) meridional surface stress in the Bering Strait, (**b**) sea ice concentration in the western Chukchi Sea, and (**c**) surface temperature in the western Chukchi Sea. The gray shading indicates the period 1980–2020. Black, red, and blue lines indicate the ALL, GHG, and AAER simulations in CESM2, respectively.

(Fig. 3c, d). The consistent dipole pattern in the linear effect suggests that feedback mechanisms are not as important to the atmospheric circulation change as it does to SIC loss. In the nonlinear effect, the weakened anticyclone in the North Pacific and the absence of a clear dipole pattern indicate overall warming manifest as low pressure in the polar region. Nonetheless, in the Chukchi Sea, the results in circulation trends are consistent with the sea ice trend.

The decomposition methodology applied in Fig. 3 assumes that the linear effect reflects the direct combined forcing from GHGs and AAER, while nonlinear effects encompass both natural variability and feedback mechanisms beyond simple GHG and AAER forcing. Although this simplified approach cannot fully separate the complex interactions between anthropogenic forcings and nonlinear feedbacks, which would require dedicated CESM2 simulations isolating GHG and AAER forcings, it provides valuable initial insights that can help shape the direction of future modeling experiments. Additionally, future research should expand beyond the western Chukchi Sea to explore how the relative influence of GHG, AAER, and nonlinear effects varies across other key Arctic regions. Such spatially comprehensive analyses would offer deeper insight into the heterogeneous nature of Arctic climate responses to anthropogenic forcings.

Temporal changes in Bering Strait surface stress and Western Chukchi Sea conditions

We plot the time series of meridional surface stress in the Bering Strait, smoothed with a 20-year running mean to reduce interannual noise (Fig. 4a). The meridional surface stress remained relatively constant prior to 1980 in both the All and AAER simulations, but from 1980 to 2020, there is a rapid increase in northward surface stress in these two simulations. The rapid increase in northward wind stress after 1980 suggests that its impact on Arctic sea ice and temperature became increasingly important during this period. In contrast, the GHG simulation shows no significant trend in meridional surface stress over the entire period, indicating that greenhouse gases alone do not significantly contribute to strong meridional exchanges of momentum or heat flux, hence lacking systematic changes in surface wind stress in the Bering Strait.

Notably, interdecadal variation is present. The period from 1980 to 2020 corresponds with a significant reduction in AAER emissions over Europe and North America, alongside a marked increase in emissions over Asia (Fig. S10), reflecting the global economical developments[24]. This spatial shift in aerosol emissions suggests that recent changes in circulation patterns and wind stress in the Bering Strait are primarily due to Asian anthropogenic aerosols, which impact climate by creating regional temperature imbalances through aerosol-radiation and cloud interactions. An increase in aerosols over East Asia coupled with a decrease in aerosols over Europe and North America induces a cooling trend in East Asia and warming trend in high latitudes. This reduced meridional temperature gradient directly weakens the midlatitude westerly flow[25], generating stationary Rossby waves that shift pressure systems and storm tracks[22]. Likewise, East Asian aerosols weaken the Aleutian Low by generating Rossby wave trains that propagate into the North Pacific, altering atmospheric circulation patterns[26]. These broader circulation adjustments subsequently manifest as an increased sea level pressure anomaly across the North Pacific. Therefore, it is likely that AAER from Asia has played a crucial role in shaping the recent circulation and wind stress patterns in the Bering Strait, contributing to regional sea ice loss in the western Chukchi Sea.

In the time series of sea ice concentration and surface temperature, the AAER simulation shows a cooling effect, while the GHG simulation shows a warming effect throughout the entire period from 1850 to 2050 (Fig. 4b, c). Interestingly, the time series in the All simulation for the period 1980–2020, which includes both GHG and AAER forcings, shows more rapid sea ice loss and warming than the GHG simulation. If only GHG and AAER forcings were acting in the All simulation, this level of sea ice decline would not occur. One would expect the sea ice concentration and surface temperature trends to be smaller than those caused by greenhouse gases or at least show the same trend. Therefore, the faster sea ice loss and warming in the All simulation compared to the GHG simulation suggest that additional feedbacks are involved. This highlights that the synergy between external forcing and feedback effects is key to explaining Chukchi Sea change, due to the pronounced AAER contribution through the atmospheric dynamics.

Relationship between Bering Strait surface stress and Western Chukchi Sea ice

The relationship between meridional surface stress in the Bering Strait and sea ice concentration in the western Chukchi Sea was further investigated using scatter plots (Fig. 5). To quantify the changes, we compared meridional surface stress and sea ice concentration between two periods (1960–1980 and 2010–2030) in the All, GHG, and AAER simulations. Each point in the scatter plots represents the changes in sea ice concentration corresponding to changes in meridional surface stress. Figure 5 reveals a significant negative relationship between meridional surface stress in the Bering Strait and sea ice concentration in the western Chukchi Sea across the All, GHG, and AAER simulations. In particular, the change in Bering Strait meridional surface stress explains 46% of the western Chukchi Sea ice concentration change in the AAER simulation. These results suggest that stronger northward surface stress is generally associated with a decline in sea ice concentration.

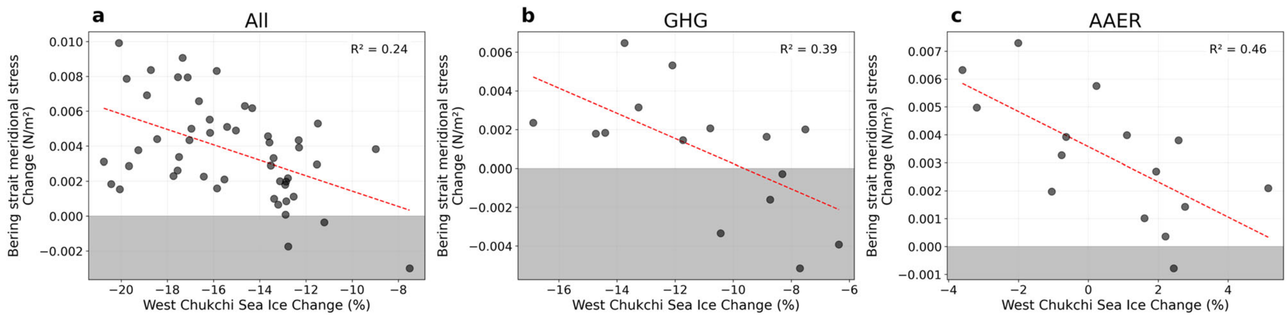

Fig. 5 | Relationship between Bering strait meridional surface stress and West Chukchi Sea ice. Scatter plots of Bering Strait meridional surface stress change versus western Chukchi Sea ice concentration change. The changes are calculated as the difference between 2010 and 2030 and 1960–1980. **a** ALL, **b** GHG, and **c** AAER simulations. Red dashed line shows the linear regression line. The negative change of surface stress is shaded by gray.

Discussion

This study demonstrates that the western Chukchi Sea ice exhibits distinct responses to AAER forcing. Unlike the widespread sea ice loss driven by GHG, the AAER simulation shows a weak yet noticeable sea ice decline in the western Chukchi Sea, suggesting that northward surface stress from AAER offsets the typical cooling effect of aerosols and ends up enhancing sea ice loss in this region. Our results further show that the combined effects of GHG and AAER shape the dominant dipole circulation pattern of change during the recent period, with an anticyclone over the North Pacific and a cyclone over the Arctic. The similarity between AAER-induced circulation and atmospheric blocking patterns emphasizes the importance of aerosols in the Pacific side of Arctic dynamics, delaying sea ice advance in the Chukchi Sea[17] through ocean heat transport caused by northward surface stress.

In the GHG-warming environment, this process further accelerates sea ice loss in the western Chukchi Sea. In contrast to the isolated effects of AAER, which intuitively affect local climate by reflecting incoming solar radiation and lead to surface cooling, the combined influence of AAER and GHGs results in the opposite effect on Arctic sea ice. This counterintuitive outcome can be explained by the interaction of two key mechanisms: (1) the background warming induced by GHGs, which increases ocean temperatures as well, and (2) the AAER-induced anticyclonic circulation anomaly over the North Pacific through atmospheric teleconnection. In this globally warmed ocean environment, the intensified anticyclonic circulation drives the northward movement of warmer ocean waters toward the Chukchi Sea. This transport of warm water ultimately outweighs the direct surface cooling effect typically associated with AAER alone. Our finding underlines the compound effect, where AAER-induced circulation change, acting in a GHG-driven warming Arctic, can exacerbate the decline in sea ice concentration. The dipole circulation pattern driven by AAER, which leads to poleward ocean heat transport throughout the Bering Strait, could serve as one of the mechanisms contributing to sea ice loss, among various others.

CESM2 limitations in sea ice dynamics and Bering Strait heat transport may affect our AAER impact quantification. High-resolution simulations show ~4× greater Bering Strait transport than standard models[27], suggesting our results potentially underestimate aerosol effects on Chukchi Sea ice loss. Our analysis indicates a potential AAER-sea ice relationship through circulation changes, though improved model physics would better characterize this relationship's magnitude and spatial extent. Moreover, a notable limitation of our study lies in the application of a linear additive approach for partitioning the effects of different forcing agents. This methodology potentially oversimplifies the complex interactions between these forcings that remain incompletely characterized in our current study. Future investigations should explicitly design experiments to quantify these interaction effects and enhance our mechanistic understanding of compound forcing responses. These insights will be instrumental in refining climate models and improving the robustness of Arctic sea ice projections. To comprehensively quantify the contribution of individual external forcings to Arctic climate change in a warming world, carefully designed sensitivity experiments are essential.

Methods

Data

We used the fifth-generation European Center for Medium-Range Weather Forecasting (ECMWF) reanalysis (ERA5) dataset from 1980 to 2020, which provides high-resolution historical climate data. To investigate future climate evolution, we utilized climate model projections. Despite substantial progress, current climate models still struggle to accurately simulate the region's rapid warming, primarily due to their limited ability to fully represent the complex local and remote processes influencing AA. Many models in the Coupled Model Intercomparison Project phase 6 (CMIP6) underestimate the sensitivity of Arctic sea ice loss to global temperature rise[2]. This shortfall stems from challenges in accurately simulating sea ice dynamics, atmospheric circulation interactions, and the role of ocean heat transport. CESM2 reasonably represents ocean heat transport through Arctic gateways, including the Bering Strait[28], making it a reliable model for assessing the impact of ocean heat transport on sea ice loss. In addition, CESM2 ranks within the top 10% of CMIP-class models in simulating large-scale circulation features including storm tracks, stationary waves, and winter blocking[29]. These features are considered relevant to Arctic sea ice variability, which supports the model's suitability for our analysis.

CESM2 Large Ensemble Community Project (LENS2)

The Community Earth System Model 2 (CESM2) Large Ensemble Project (LENS2), developed by the National Center for Atmospheric Research (NCAR), is utilized in this study because its large ensemble size allows for a clearer separation of external and internal forcings[30]. We use 50 ensemble members from the CESM2 Large Ensemble, referred to as the "All" simulation in this study. Additionally, to estimate the effects of individual forcings on the Arctic, we use data from the CESM2 Single Forcing Large Ensemble Project. Specifically, we utilize 15 ensemble members from the greenhouse gases evolving (GHG) simulation and the anthropogenic aerosols evolving (AAER) simulation. These simulations use the same model and external forcings as the CESM2 Large Ensemble Project. The difference in the number of ensemble members between the All simulation and the GHG and AAER simulations did not significantly impact the results in this study (Fig. S11). The All simulation covers the period 1850–2100 under the CMIP6 historical and SSP370 future radiative forcing scenarios. The GHG and AAER simulations cover the period 1850–2050 and follow the "only" method for single forcing experiments, meaning all other forcings are held fixed at their 1850 levels while only the target forcing (either GHG or AAER) evolves over time.

Statistic

In this study, all variables are based on annual mean and annual trend. We define the following regions: the Bering Strait (170–210°E, 65–75°N), the western Chukchi Sea (150–190°E, 70–75°N). For the time series of ensemble means of sea ice concentration, surface temperature, and meridional surface stress, we applied a 20-year running mean to reduce interannual noise (Fig. 4). The anomalies were calculated by subtracting the climatology of the period prior to 1900.

Variance partitioning analysis

The combined effect of GHG and AAER forcings was calculated by summing the respective single-forcing simulations with an initial offset correction to ensure proper alignment with the ALL forcing simulation. This offset correction accounts for differences at first year of analysis and baseline states between simulations:

$$offset = SIC_{ALL,first\ year} - (SIC_{GHG,first\ year} + SIC_{AAER,first\ year}) \quad (1)$$

The combined time series was then computed as:

$$SIC_{GHG+AAER} = SIC_{GHG} + SIC_{AAER} + offset \quad (2)$$

This approach maintains consistent reference points while preserving the independent temporal evolution and relative contributions from each forcing component.

The explanatory capability of each simulation was evaluated by calculating the coefficient of determination (R^2) between each simulation and the ALL simulation:

$$R^2 = \frac{[cov(SIC_{simulation}, SIC_{ALL})]^2}{var(SIC_{simulation}) \times var(SIC_{ALL})} \quad (3)$$

The relative increase in explained variance was calculated to quantify the improvement gained by incorporating aerosol effects alongside greenhouse gas forcing:

$$Relative\ increase\ in\ explained\ variance = \frac{(R^2_{GHG+AAER} - R^2_{GHG})}{R^2_{GHG}} \times 100\% \quad (4)$$

This metric represents the percentage improvement in explanatory capability when both forcings are considered together compared to GHG forcing alone.

To assess the actual magnitude of variance captured, the percentage of total variance explained was calculated as:

$$Percentage\ of\ ALL\ variance = \frac{var(SIC_{simulation})}{var(SIC_{ALL})} \times 100\% \quad (5)$$

This metric provides direct quantification of how much of the total sea ice concentration variability in the ALL forcing simulation is reproduced by the individual forcing simulations and their combination.

Analysis approach

We partition the existing simulations into two components: the linear effect and the nonlinear effect. The linear effect is defined as the sum of the simulations forced individually by GHG and AAER. The nonlinear effect is then calculated by subtracting this sum from the ALL simulation, which includes all external and internal forcings. The assumption is that the linear effect represents the combined influence of external forcings from GHG and AAER, while the nonlinear effect captures natural forcings and other feedback mechanisms not accounted for by GHG and AAER alone. Although this simplistic approach does not fully decompose the combined effects of anthropogenic agents or nonlinear feedbacks—which would ideally require separate CESM2 runs with only GHG and AAER as forcings to show their true effects—it serves as a preliminary analysis that can inform and guide future modeling studies.

Data availability

The ERA5 and CESM2 LENS are available at https://cds.climate.copernicus.eu and http://earthsystemgrid.org, respectively. Derived data generating the figures of this study are available from Zenodo at https://zenodo.org/records/15858967.

Code availability

The source codes for the analysis of this study are available from the corresponding author upon reasonable request.

Received: 3 January 2025; Accepted: 11 July 2025;
Published online: 25 July 2025

References

1. Cohen, J. et al. Divergent consensuses on Arctic amplification influence on midlatitude severe winter weather. *Nat. Clim. Change* **10**, 20 (2020).
2. Rantanen, M. et al. The Arctic has warmed nearly four times faster than the globe since 1979. *Commun. Earth Environ*. **3**, 168 (2022).
3. Wu, Y. T. et al. Exploiting SMILEs and the CMIP5 archive to understand arctic climate change seasonality and uncertainty. *Geophys. Res. Lett*. **50**, e2022GL100745 (2023).
4. Screen, J. A. & Simmonds, I. The central role of diminishing sea ice in recent Arctic temperature amplification. *Nature* **464**, 1334–1337 (2010).
5. Vavrus, S. The impact of cloud feedbacks on Arctic climate under greenhouse forcing. *J. Clim.* **17**, 603–615 (2004).
6. Beer, E. & Eisenman, I. Revisiting the role of the water vapor and lapse rate feedbacks in the arctic amplification of climate change. *J. Clim.* **35**, 2975–2988 (2022).
7. Doerr, J., Arthun, M., Eldevik, T. & Sando, A. B. Expanding influence of Atlantic and Pacific Ocean heat transport on winter sea-ice variability in a warming Arctic. *J. Geophys. Res. Oceans* **129**, e2023JC019900 (2024).
8. Serreze, M. C. & Barry, R. G. Processes and impacts of Arctic amplification: a research synthesis. *Glob. Planet Change* **77**, 85–96 (2011).
9. Goosse, H. et al. Quantifying climate feedbacks in polar regions. *Nat. Commun.* **9**, 1919 (2018).
10. Graversen, R. G., Langen, P. L. & Mauritsen, T. Polar amplification in CCSM4: contributions from the lapse rate and surface Albedo feedbacks. *J. Clim.* **27**, 4433–4450 (2014).
11. Årthun, M., Eldevik, T. & Smedsrud, L. H. The role of Atlantic heat transport in future Arctic Winter Sea ice loss. *J. Clim.* **32**, 3327–3341 (2019).
12. Polyakov, I. V. et al. Greater role for Atlantic inflows on sea-ice loss in the Eurasian Basin of the Arctic Ocean. *Science* **356**, 285 (2017).
13. Polyakov, I. V. et al. Borealization of the Arctic Ocean in response to anomalous advection from sub-arctic seas. *Front. Mar. Sci*. **7** (2020).
14. Danielson, S. L. et al. Manifestation and consequences of warming and altered heat fluxes over the Bering and Chukchi Sea continental shelves. *Deep Sea Res. Pt Ii* **177**, 104781 (2020).
15. Wang, M. Y., Overland, J. E. & Stabeno, P. Future climate of the Bering and Chukchi Seas projected by global climate models. *Deep Sea Res. Pt Ii* **65-70**, 46–57 (2012).
16. Docquier, D., Koenigk, T., Fuentes-Franco, R., Karami, M. P. & Ruprich-Robert, Y. Impact of ocean heat transport on the Arctic sea-ice decline: a model study with EC-Earth3. *Clim. Dynam.* **56**, 1407–1432 (2021).
17. Kodaira, T., Waseda, T., Nose, T. & Inoue, J. Record high Pacific Arctic seawater temperatures and delayed sea ice advance in response to episodic atmospheric blocking. *Sci. Rep.* **10**, 20830 (2020).
18. Polyakov, I. V. et al. Atmospheric pressure rivalry between the Arctic and Northern Pacific: implications for Alaskan climate variability. *Int J. Climatol.* **44**, 5339–5357 (2024).

19. Smedsrud, L. H. et al. The role of the Barents Sea in the Arctic Climate System. *Rev. Geophys.* **51**, 415–449 (2013).
20. Serreze, M. C., Crawford, A. D., Stroeve, J. C., Barrett, A. P. & Woodgate, R. A. Variability, trends, and predictability of seasonal sea ice retreat and advance in the Chukchi Sea. *J. Geophys. Res. Oceans* **121**, 7308–7325 (2016).
21. Dittus, A. J., Hawkins, E., Robson, J. I., Smith, D. M. & Wilcox, L. J. Drivers of recent North Pacific decadal variability: the role of aerosol forcing. *Earths Future* **9**, e2021EF002249 (2021).
22. Wilcox, L. J. et al. Mechanisms for a remote response to Asian anthropogenic aerosol in boreal winter. *Atmos. Chem. Phys.* **19**, 9081–9095 (2019).
23. Liu, W., Fedorov, A. V., Xie, S. P. & Hu, S. N. Climate impacts of a weakened Atlantic Meridional Overturning Circulation in a warming climate. *Sci. Adv.* **6**, eaaz4876 (2020).
24. Pozzer, A. et al. Effects of business-as-usual anthropogenic emissions on air quality. *Atmos. Chem. Phys.* **12**, 6915–6937 (2012).
25. Smith, D. M. et al. Role of volcanic and anthropogenic aerosols in the recent global surface warming slowdown. *Nat. Clim. Change* **6**, 936 (2016).
26. Dow, W. J., Maycock, A. C., Lofverstrom, M. & Smith, C. J. The effect of anthropogenic aerosols on the Aleutian Low. *J. Clim.* **34**, 1725–1741 (2021).
27. Xu, G. P. et al. High-resolution modelling identifies the Bering Strait's role in amplified Arctic warming. *Nat. Clim. Change*. **14** (2024).
28. Oldenburg, D. et al. The respective roles of ocean heat transport and surface heat fluxes in driving Arctic Ocean Warming and Sea Ice Decline. *J. Clim.* **37**, 1431–1448 (2024).
29. Simpson, I. R. et al. An evaluation of the large-scale atmospheric circulation and its variability in CESM2 and other CMIP models. *J. Geophys. Res. Atmos*. **125** (2020).
30. Rodgers, K. B. et al. Ubiquity of human-induced changes in climate variability. *Earth Syst. Dynam.* **12**, 1393–1411 (2021).

Acknowledgements
This research is funded by the National Research Foundation of Korea (NRF-2021R1A2C1011827 and RS-2025-02363044), and by the Korea Environment Industry & Technology Institute (KEITI) through "Climate Change R&D Project for New Climate Regime", funded by Korea Ministry of Environment (MOE) (RS-2022-KE002160). Shih-Yu Wang was supposed by the NCHU-KU Joint Research Project, Grant Number 00062024.

Author contributions
Yungi Hong: investigation, visualization, analysis, writing-original draft, reviewing, and editing. Shih-Yu (Simon) Wang: conceptualization, writing, reviewing, editing, and supervision. Jin-Ho Yoon: conceptualization, investigation, writing, reviewing, editing, supervision, and funding acquisition.

Competing interests
The authors declare no competing interests.

Additional information
Supplementary information The online version contains supplementary material available at https://doi.org/10.1038/s43247-025-02577-7.

Correspondence and requests for materials should be addressed to Jin-Ho Yoon.

Peer review information *Communications Earth & Environment* thanks Judah Cohen and the other anonymous reviewer(s) for their contribution to the peer review of this work. Primary Handling Editors: Yinon Rudich and Alice Drinkwater. [A peer review file is available].